Applications of predictions for FRC translation to MTF

T. P. Intrator*

Los Alamos National Laboratory, M.S. E526, Los Alamos, NM 87545, USA

R.E. Siemon

Department of Physics, Univ Nevada - Reno

P. E. Sieck

Los Alamos National Laboratory

(Dated: August 17, 2007)

We describe a physics scaling model used to design the high density Field Reversed Configuration (FRC) at LANL that will translate into a mirror bounded compression region, and undergo Magnetized Target Fusion compression to a High Energy Density plasma. The theta pinch formed FRC will be expelled from inside a conical theta coil. At Kirtland AFRL the FRC will be compressed inside a flux conserving cylindrical shell. Semi empirical scaling laws, which were primarily developed and benchmarked for collisionless Field Reversed Configurations (FRC) are expected to remain valid even for the collisional regime of FRXL experiment. The scaling laws are used to predict the the time available for the translation compared to the lifetime of the FRC. This approach is used to outline the design and fabrication of the integrated MTF plasma compression experiment.

PACS numbers:

I. INTRODUCTION

Intrinsically pulsed approaches to fusion energy include Magneto Inertial Fusion (MIF) that takes advantage of magnetically enhanced confinement (Kirkpatrick et al., 1995)., and Magnetized Target Fusion (MTF) that compresses a plasma target with closed magnetic surfaces. The FRX-L experiment at at Los Alamos National Laboratory (LANL) is implementing translation of a Field Reversed Configuration (FRC) from a formation region into a location where it can be compressed and adiabatically heated to fusion relevant conditions inside of a converging and flux conserving boundary. A high pressure FRC target plasma should be sufficiently robust to undergo compression, and has already been shown(Intrator et al., 2004a) (Zhang et al., 2006) to possess adequate density and temperature for the physics premises of an MTF target(Siemon et al., 1999)(Intrator et al., 2004b).

We describe a simple physics scaling model that is used for the design for a high density FRC with translation. The translation is expected to lead to increased trapped bias flux during formation, and therefore increased FRC lifetime, as well as facilitate study of the FRC internal structure. These results are intended to enhance the MTF parallel experiment at Kirtland Air Force Research Laboratory (AFRL), where a simpler version with fewer diagnostics is being constructed to implode and FRC within a flux conserving cylindrical shell.

II. FRC TRANSLATION

Translation of an FRC confers some significant advantages. It offers an engineering convenience for several CT fusion reactor studies in which startup, heating and burn chamber technologies can be spatially separated and independently optimized. Expensive crowbar systems for theta coil pulsed power systems become no longer necessary. Vacuum coupled diagnostics such as VUV and SXR spectroscopy, bolometry, internal magnetic probes, auxiliary heating or current drive schemes become much easier to implement in a translation region rather than a theta coil formation region. Axial profiles are accessible in a straightforward manner as the FRC transits past each diagnostic field of view. Translation over a pellet may enable novel fueling methods. Translation into a flux conserver with reduced radius may increase the FRC size compared to the ion gyro radius, i.e. increase the value of s, where $s = \int_{R_0}^{r_s} rdr/(r_{Gi} r_s)$, r_{Gi} is the local ion gyro radius, r_s is the separatrix radius, and R_0 is the magnetic null radius.

Successful FRC translation has been demonstrated in several experiments. A conical theta coil was used in FRX-C (Rej et al., 1986), and many other experiments. Fast pulsed mirrors were used in FRX-A (Armstrong et al., 1981), and sequentially triggered coils in TRX experiments (Slough and Hoffman, 1997). Pulsed and sequential magnets have the advantage that one can control the formation separately from the translation timing, but have the disadvantage of requiring numerous high voltage pulsed magnet circuits. We will choose the conical theta coil option.

*Electronic address: `intrator@lanl.gov`

III. FRC TRANSLATION FOR MTF

Predictions of performance rely on existing measurements of the FRXL plasma parameters. It takes advantage of a LANL tested (Intrator et al., 2004a) formation scenario and technology. The simplest scheme with the lowest technology requirements is to use a conical theta coil to form and eject the FRC. The cone angle also imparts helicity and robustness to the FRC(Wira and Pietrzyk, 1990) (Guo et al., 2005).

For our existing formation scheme, the translation speed must be slow enough so the FRC escapes from the formation region in a time comparable or longer than the formation time. To minimize FRC lifetime requirements the translation time must be as fast as practicable.

In order to approximate the formation and translation as approximately adiabatic, *i.e.* energy is approximately conserved in the FRC, we need to translate the FRC out of the formation region in a time comparable to or longer than important scale times. These include the formation $\tau_{for} \approx 3\mu$sec time, ion-ion collision time $\tau_{ii} \approx 50 - 100$nsec and axial bounce frequency time $\tau_b = z_s/v_A \leq 2\mu$sec, where z_s is the half length of the separatrix, and v_A is the Alfven speed. For FRXL $\tau_{for} \approx 3\mu$sec.

Semi empirical scaling laws (Spencer et al., 1983; Tuszewski, 1988a), which were primarily developed and benchmarked for collisionless FRC's are expected to remain valid even for the collisional regime of FRXL experiment. This equilibrium model is presumed to be valid after a violent formation stage that is usually assumed to be cylindrically symmetric (i.e. not conical) along the z axis as seen in figure 1.

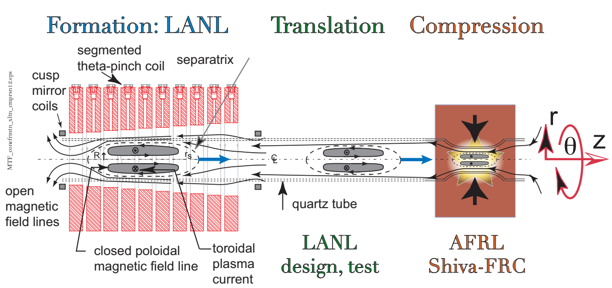

FIG. 1 Schematic of the formation, translation, and compression regions, including coordinate system. Note that the magnetic field is largest at the small end of the conical theta coil, and decreases to a smaller average value in the translation region.

Ultimately, characterization of the translating plasma will require diagnoses of FRC during formation, translation, and the behavior in both the fake liner implosion region at LANL, and the real implosion at AFRL. This includes evaluation of particle, energy, and flux confinement in these regions along with stability and confinement lifetimes.

IV. THERMODYNAMICS OF COMPRESSION AND DECOMPRESSION

A. Adiabatic approach

The simplest model of plasma evolution is an adiabatic model, where the FRC posesses a total poloidal magnetic flux Ψ and internal pressure profiles $p(\psi)$ that are a function of local ψ. This is equivalent to presuming that the plasma evolves through a sequence of isentropic magnetohydrodynamic (MHD) equilibria, *i.e.* each is constrained to contain the same entropy per unit flux, because no heat goes into or out of the FRC separatrix. This is a thermodynamic approach that only accounts for initial and final states and omits dynamics. A way of computing such equilibria was developed by Grad (Grad et al., 1975), and later applied to FRC's (Byrne and Grossmann, 1980).

The FRC behavior for this purpose can be characterized by

- wall or flux conserver radius r_c
- Ratio of the guide field B_g past the ends of the FRC (determines the flux outside the FRC) to the average magnetic field in the formation theta coil.
- separatrix radius r_s or $x_s = r_s/r_c$
- plasma density maximum at the field null

We will use the adiabatic model outlined by Spencer (Spencer et al., 1983), (Tuszewski, 1988a) along with a translation model derived by Ohi (Tanjyo et al., 1984) that was benchmarked on FRX-C (Rej et al., 1986) and other FRC experiments.

B. FRC compression and decompression

Elongated FRC equilibria can be reasonably well described using two regions with straight field lines connected by a short transition region with curved field lines.(Hewett and Spencer, 1983).This property enables one to extract two dimensional information from a one dimensional calculation for elongations of $l_s/r_s > 8$, where l_s is the total length of the straight field lines and r_s is the separatrix radius.

Since flux ψ is conserved, the flux tube volume inside a contour C is

$$V_\psi = \psi \left(\oint_C \frac{dl}{B} \right) \tag{1}$$

where the line integral is carried out over closed field lines. The adiabatic equation of state is

$$pV^\gamma = \mu = constant \tag{2}$$

where $\gamma = (n_{dof} + 2)/n_{dof}$ is a polytropic index and n_{dof} counts the degrees of freedom. The entropy per unit flux for a flux tube is

$$\mu(\psi) = p(\psi)\left(\oint \frac{dl}{B}\right)^{\gamma} \tag{3}$$

We consider a prolate elongated FRC that is confined with a conducting cylinder of average radius r_c as shown in figure 1. The magnetic flux outside the separatrix is ψ_0 and inside the separatrix is ψ. The pressure profile $p(\psi)$ vanishes outside the separatrix $r = r_s$ and has a maximum p_m at the magnetic axis $r = R_0 = r_s/\sqrt{2}$. We will not account for pressure outside the separatrix $r > r_s$.

The radial force balance can be written

$$p(\psi) + \frac{B(\psi)^2}{2\mu_0} = \frac{B_{eq,w}^2}{2\mu_0} \tag{4}$$

where $B_{eq,w}$ is the compressed equilibrium magnetic field between the FRC and the coil. The approximation that makes this model one dimensional is

$$\oint \frac{dl}{B} \approx \frac{2l}{B} = \frac{2l}{[2(p_m - p(\psi)]^{1/2}} \tag{5}$$

This approximation is wrong at the O-point and separatrix, but has been shown to behave well for volume averaged quantities (Spencer et al., 1983).

The combination of radial and axial force balance (see *e.g.* (Barnes et al., 1979), (Armstrong et al., 1981)) constrains the volume averaged beta to be a function of x_s the normalized separatrix radius

$$\langle\beta\rangle = 1 - x_s^2/2 \tag{6}$$

where

$$\langle\beta\rangle = \frac{2}{R_0^2}\int_0^{R_0} \frac{p(r)}{p_m} r dr = \int_0^1 \beta(u) du \tag{7}$$

and flux quantities such as $p(r)$ are symmetric in $u = r^2 - R_0^2$.

C. Adiabatic flux compression scaling

Adiabatic compressions of the idealized cylindrical FRC can occur either via changes in wall compression r_c or flux compression ψ_0. Since the arguments are thermodynamic, they are robust, and also have been verified on both US (Rej et al., 1986) and Japanese (Tanjyo et al., 1984) (Himura et al., 1994) experiments. The down-stream conducting boundary is essential if we want to translate with the familiar FRC equilibrium because eddy currents in the wall must be able to move when the FRC moves. We will assume that during translation the FRC is in a region surrounded by a conducting wall of radius r_c containing a uniform guide field of magnitude B_g.

Within the separatrix there is a balance between internal energy E and work W done on the separatrix which can be written as $dE = dW$. The total energy within the separatrix volume is

$$E = \int \left(\frac{p}{\gamma - 1} + \frac{B^2}{2\mu_0}\right) dV \tag{8}$$

and using the Barnes relation equation 7 it can be shown that

$$E = p_m V \frac{1 - (2-\gamma)x_s^2/2}{\gamma - 1} \tag{9}$$

The work done on the separatrix by the external magnetic field pressure can be calculated (Spencer et al., 1983) from the differential dW for the two cases of flux and boundary compression. If one assumes that changes in pressure profile $\beta(u)$ follow only from variations in x_s, and that the profile index ϵ does not vary with x_s, then scaling laws can be deduced (Spencer et al., 1983) that do not depend on the details of the pressure profile.

A profile index ϵ is typically used to characterize the trapped poloidal flux in the FRC. The high flux sharp boundary corresponds to $\epsilon = 0$, and $\epsilon = 1$ to the low flux sharp boundary. Consistent with past experience and the FRC literature (Tuszewski, 1988b) (Tuszewski, 1988a) , we invoke $\epsilon = 0.25$, *i.e.* closer to the high flux sharp boundary case. The normalized separatrix radius is $x_s = r_s/r_c$.

TABLE I Scaling predictions for compressed FRC's. Note that z_s is the half separatrix length and $2z_s = l_s$, n_m is the maximum density at $r = R_0$, T is the temperature which is assumed to be constant in r.

parameter	ϵ scaling (adiabatic only)
x_s	
$2z_s$	$x_s^{2(4+3\epsilon)/5}\langle\beta\rangle^{-(3+2\epsilon)/5} r_c^{2/5}$
z_s/r_s	$x_s^{3(1+2\epsilon)/5} r_c^{7/5}$
n_m	$x_s^{-6(3+\epsilon)/5}\langle\beta\rangle^{-2(1-\epsilon)/5} r_c^{-12/5}$
T	$x_s^{-4(3+\epsilon)/5}\langle\beta\rangle^{2(1-\epsilon)/5} r_c^{-8/5}$
$B_{eq,w}$	$x_s^{-(3+\epsilon)} r_c^{-2}$
$\langle\beta\rangle$	$1 - x_s^2/2$

Table I shows the scaling relations that follow from the foregoing discussion, and relate most relevant FRC quantities to x_s.

Although the relationships are not linear, if one specifies a new value for x_s, then there is a corresponding changed relationship between applied magnetic field B_z and equilibrium field $B_{eq,w}$. Conversely if B_z or $B_{eq,w}$ is changed x_s must vary.

We wish to model liner compression for MTF, where the flux in the FRC is held constant and the flux between the conducting wall and the FRC is also held constant, so that x_s remains constant.

Thus adiabatic compression or decompression of an FRC is neatly written in terms of two independent variables, x_s and flux conserving boundary radius r_c. Translation is viewed as a combination of flux compression and wall compression because both variables can be changed in the process. These equations ignore pressure effects on the open field lines and treat the FRC as a magnetic bladder with plasma pressure inside the separatrix. They also ignore plasma rotation and other stability issues.

D. External field compression in equilibrium

The initial guide field is squeezed against the wall because the FRC excludes flux as it travels down its flux conserving container. The external magnetic field outside the FRC between the wall and the FRC is

$$B_{eq,w} = \frac{B_z}{1 - x_s^2} \tag{10}$$

The guide field B_g that is created by the external magnets is smaller than the equilibrium field, but it determines the engineering figures of merit needed to design the magnets and circuits. Therefore we will use the ratio of applied vacuum magnetic fields B_{z2}/B_{z1}, where subscripts 1(2) refer to the formation(translation) regions.

We shall later find it useful to estimate the total internal poloidal flux. The equilibrium constraint and integration of poloidal flux for the domain $0 < r < R_0$ or equivalently $R_0 < r < r_s$ yields the relation

$$\phi_p = \pi r_c^2 B_{eq,w} \left(\frac{x_s}{\sqrt{2}}\right)^{3+\epsilon} \tag{11}$$

$$= \pi R_0^2 B_{eq,w} \left(\frac{R_0}{r_c}\right)^{1+\epsilon} \tag{12}$$

Where r_c is the flux conserving coil radius, and the normalized magnetic null radius is $R_0/r_c = x_s/\sqrt{2}$. $B_{eq,w}$ is measured experimentally, and r_s is determined from this plus an excluded flux measurement (Tuszewski, 1981). On the right hand side of equation 12, the left hand term is an equivalent flux inside the magnetic null referenced to the magnetic field $B_{eq,w}$ outside the separatrix, *i.e.* as if the FRC had zero magnetic moment. The right hand term accounts for the diamagnetism of the FRC, which reduces this equivalent flux.

In terms of table I, B_{z2}/B_{z1} determines the ratio of the separatrix radii which can then be used to predict the β and all the other parameters.

$$\frac{x_{s2}}{x_{s1}} = \left\{ \frac{B_{z1}}{B_{z2}} \frac{1 - x_{s2}^2}{1 - x_{s1}^2} \left(\frac{r_{c2}}{r_{c1}}\right)^2 \right\}^{\frac{1}{3+\epsilon}} \tag{13}$$

The solution is most easily solved numerically for B_{z1}/B_{z2} as a function of x_{s2}/x_{s1}, which we have done for figure 2.

$$\frac{B_{z1}}{B_{z2}} = \left(\frac{x_{s2}}{x_{s1}}\right)^{3+\epsilon} \frac{1 - x_{s2}^2}{1 - x_{s1}^2} \left(\frac{r_{c2}}{r_{c1}}\right)^2 \tag{14}$$

The values of r_{c1} and r_{c2} allow for the possibility of different flux conserver radii for formation and translation regions.

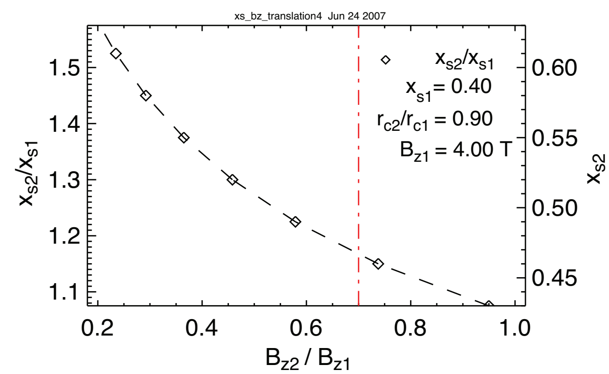

FIG. 2 adiabatic and flux conserving predictions for separatrix radius. Note that the FRC expands (x_s increases as the magnetic field in the translation region decreases.

Using the above relations, figure 2 shows the predicted separatrix radius x_{s2} as a fraction of the initial x_{s1} as a function of magnetic field decrease B_{z2}/B_{z1} using the following

$$\frac{\langle\beta_2\rangle}{\langle\beta_1\rangle} = \frac{1 - x_{s2}^2/2}{1 - x_{s1}^2/2} \tag{15}$$

$$\frac{T_2}{T_1} = \left(\frac{B_{eq,w2}}{B_{eq,w1}}\right)^{4/5} \left(\frac{\langle\beta_2\rangle}{\langle\beta_1\rangle}\right)^{2(1-\epsilon)/5} \left(\frac{r_{c1}}{r_{c2}}\right)^{16/[5(3+\epsilon)]} \tag{16}$$

The predicted values of β then depend on the reduction in B_{z2} compared with B_{z1}. and are plotted in figure 3 The predicted β from figure 3 and equation 16 allows

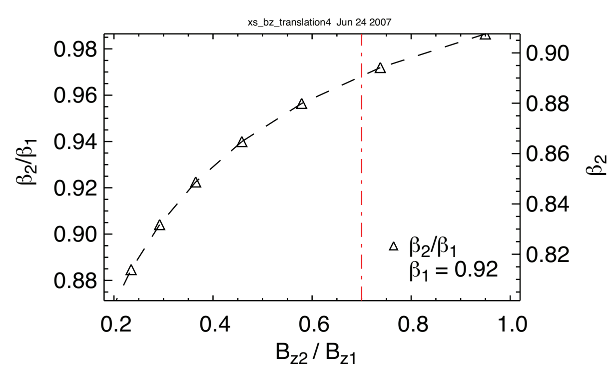

FIG. 3 adiabatic and flux conserving predictions for FRC β as a function of B_{z2}/B_{z1}

evaluation of the temperature as shown in figure 4.

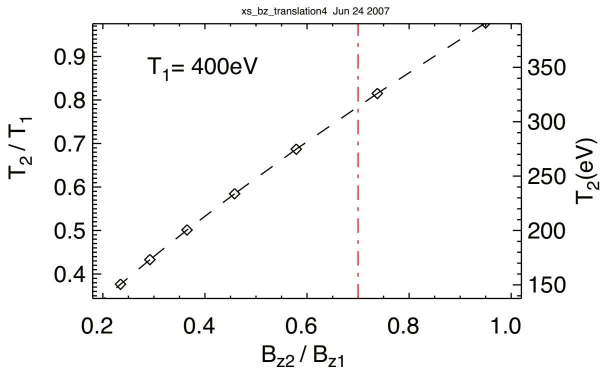

FIG. 4 adiabatic and flux conserving predictions for FRC temperature T as a function of B_{z2}/B_{z1}

The separatrix length also increases strongly with x_s. This will have the consequence that any MTF liner will need to be sufficiently long to contain the FRC as it enters the flux conserver implosion region.

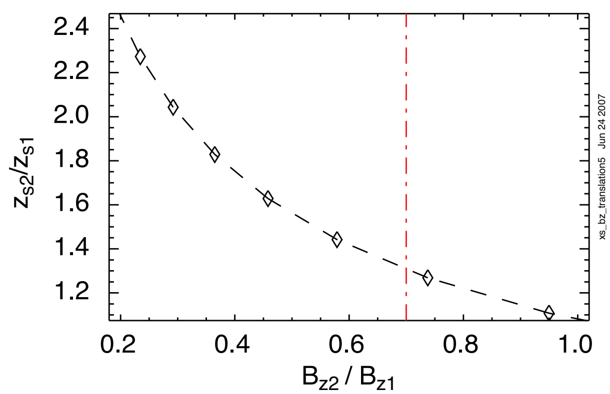

FIG. 5 adiabatic and flux conserving predictions for FRC separatrix half length z_s as a function of B_{z2}/B_{z1}

E. Translation energy

During formation the magnetic field changes rapidly in the theta pinch coil, and transfers electromagnetic energy to the plasma. After the field is crowbarred in the theta pinch near the time of maximum field, the FRC can translate, but there is no electromagnetic work being done by the fields on the plasma system (Poynting flux is zero). Voltage is zero in the theta pinch after the crowbar time, and zero around the metal surfaces that surround the FRC plasma during translation. The initial condition for the FRC in the formation coil is a small amount of translation kinetic energy resulting from the conical coil shape, plus considerably larger thermal energy resulting from the implosion.

We will consider an enthalpy quantity, which is the total energy E_T inside the metallic flux conserving volume boundaries of the experiment. The three terms on the right hand side sum the plasma thermal, axial kinetic, and magnetic field energies. Using the elongated FRC equilibrium constraints from equations 6 and 21 the total energy was first written in the form of equation 17

$$E_T = \frac{5}{2} N k_B T + N m_i v_z^2 + E_{BV} \tag{17}$$

by Ohi (Tanjyo et al., 1984). N is the ion inventory, m_i is the ion mass, k_B is the Boltzmann constant, $T = T_e + T_i$ is the total temperature, and E_{BV} is the total magnetic energy contained inside the flux conserver in the absence of the plasma. The first term on the right hand side includes thermal energy from heat capacity for 3 degrees of freedom at constant volume (VdP) plus PdV work at constant pressure, and the second term contains translational energy in the FRC. The quantity E_{BV} is the magnetic field energy in vacuum $E_{BV} = [B_{z0}^2/(2\mu_0)]\pi r_c^2 L$ where L is the length of the volume of interest. E_{BV} is an order of magnitude larger than the other terms. During the time evolution the guide field changes only slightly while the main bank is crowbarred. The energy conservation approximation was shown to be valid to $\approx$ 4% on FRX-C (Rej et al., 1986).

To within this error, the thermal plus translation energy

$$\Theta = 5 k_B T + m_i v_z^2 \tag{18}$$

remains approximately conserved over time.

During translation there can be a change in x_s and r_c. If the plasma decompresses by some amount, T drops. This is consistent with Liouville's theorem, which requires that phase space volume is conserved. The thermal energy spread for any accelerated distribution decreases as as its average velocity increases.

Using the adiabatic relationships from Table I the change in temperature can be computed. Equation 18 then requires that a drop in T be accompanied by an increase in v_z, and conserved E_T allows the translation speed to be predicted

$$v_z = \left(5 \frac{k_B \Delta T}{m_i} + \frac{2 \Delta E_{BV}}{N m_i}\right)^{1/2} \tag{19}$$

where the change in T is $\Delta T = T_1 - T_2$, and we will neglect the E_{BV} term. In other FRC experiments, the plasma has been observed to expand somewhat more and cool somewhat less than the adiabatic predictions ($\approx$ 15% discrepancy). The natural dimensionless velocity is

$$\frac{v_z}{c_{s1}} = \left(5 \frac{\Delta T}{T_1}\right)^{1/2} \tag{20}$$

The translation speed was observed on FRX-C to be limited to a value on the order of $\sqrt{5}\, c_{s1}$, which is the asymptotic upper bound on v_{z2} in figure 6. In numerical models, the scaling that follows from equation 20

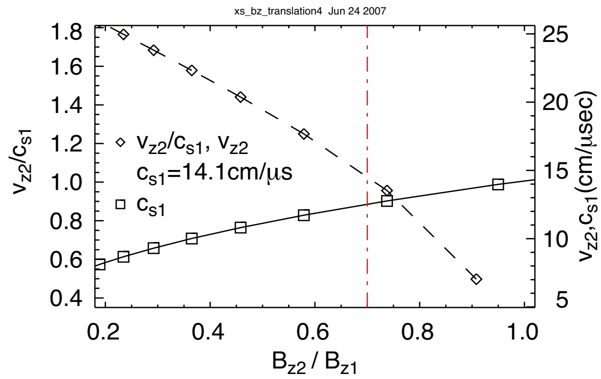

FIG. 6 adiabatic and flux conserving predictions for translation velocity

could easily be confused with a dependence on the Alfven speed. Since β is of order unity, the Alfven speed and the sound speed are not very different.

V. FRC DYNAMIC ACCELERATION

A. Translation force

For the conventional cylindrical FRC, the radial force balance can be written

$$J_{tor} \times B_{pol} - \nabla p = 0 \quad (21)$$

where J_{tor} is the toroidal plasma current density, B_{pol} is the FRC poloidal magnetic field, and p is the plasma pressure. But for the conical theta coil with B_{pol} tilted by the angle α, there is an unbalanced axial acceleration magnetic force which can be approximated as

$$F_z \approx I_{tor} \times B_{pol}\ sin(\alpha)\ 2\pi r_s \quad (22)$$

where r_s is the separatrix radius.

The conical theta coil formation and FRC expulsion from small to large area regions of the theta coil determines the degree of expansion for the FRC volume.

B. Choice of cone angle

There are conflicting requirements that must be balanced for both short and long FRC formation and expulsion times. This time scale is directly related to the optimal magnitude for the expulsion force that drives the FRC out of the theta coil.

Large force and hence short translation time reduces the need for a long FRC lifetime. On the other hand, if the conical theta coil angle that leads to this force is too large, it may eject the FRC on a faster time scale than formation. This could lead to a poorly understood dynamic formation that does not culminate in a recognizable FRC equilibrium. It might also impart too much toroidal magnetic field (Wira and Pietrzyk, 1990) (Milroy and Brackbill, 1986) and spheromak characteristics to the FRC.

Historically conical theta coils have been used to generate spheromak (Wells, 1966) (Wells et al., 1974) like plasmas (Tuszewski and Wright, 1989). A plot of predicted Φ_{tor}/Φ_{pol} vs cone angle (full cone angle = 2α) in figure 7 taken from (Wira and Pietrzyk, 1990) shows $\Phi_{tor}/\Phi_{pol} \approx 3\%$ for FRX-C parameters.

At LANL, the FRX-C experiment (Rej et al., 1986) showed that a much smaller α than previous translation experiments was sufficient to translate an FRC. FRXC had a stepped approximation fo a conical theta coil with effective cone half angle $\alpha = 1.4$ degrees), 4 sections. It was a total of 200 cm long with a length to diameter ratio of ≈ 8. The coil area at the ejection end of the theta coil was 34% larger than the other end. FRX-C

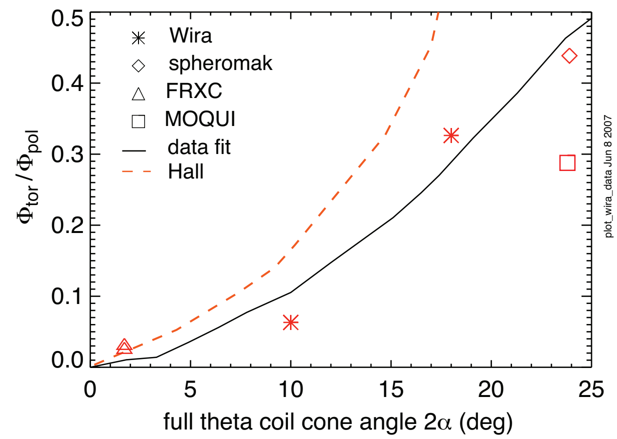

FIG. 7 Model predictions of non ideal toroidal magnetic flux in FRC, with some data points taken from figure 13 from Wira (Wira and Pietrzyk, 1990), FRXC(Chrien and Armstrong, 1984), and a spheromak merging experiment (Kawai, 1987).

translation data from a low compression mode shows a CT emerging from the formation region, bouncing several times between the far end mirror and the theta coil. That is, for $B_{bias} \approx -1$kG, formation field $B_{z1} \approx +5$kG, translation field $B_{z2} \approx +2.5$kG, these experiments would be placed on figures 2, 3, 4, 6 at a 50% reduction in field $B_{z2}/B_{z1} \approx 0.5$ between theta coil and translation regions. For a wide variety of B_{z2}/B_{z1} the reported translation speed was consistent with equation 20.

C. Formation time vs expulsion time

The FRX-C data and analyses (Rej et al., 1986) showed that if the acceleration / expulsion time was $1-2$ times the formation time, the translation proceeded well. By this we mean that the final translating FRC persisted with very similar confinement properties to the standard well formed static FRC.

We will choose an operating regime where $B_{z2}/B_{z1} \approx 0.7$ in figures 2, 3, 4, 6 to provide a peak translation speed estimated from figure 6 on the order of $v_z \approx 10 - 12$cm/μsec. The average speed will then be half of this, *i.e.* $\langle v_z \rangle \approx 5 - 6$cm/$\mu$sec. This corresponds to a conical theta coil half angle $\alpha = 2°$.

For FRXL we estimate $\tau_{acc}(FRXL) = z_{coil}/\langle v_z \rangle \approx$ 36cm/(6cm/μsec) $\approx 6\mu$sec. The formation time is approximately $\tau_{form} \approx 3\mu$sec, so that for this design point, $\tau_{acc}(FRXL) \approx 2\tau_{form}$

Dynamic formation and reconnection data due to asymmetric theta coil fields in the TRX series of experiments has favorably been compared with MOQUI code (Armstrong and Milroy, 1982) predictions. The problem was also discussed briefly by (Rej et al., 1986) for FRX-C.

VI. CONSIDERATIONS FOR MTF

A. FRC translation constraints for MTF

The FRC in the translation region experiences adiabatic expansion as the B_z field decreases, i.e. x_s will increase. The coil generated vacuum magnetic field B_{z0} will get compressed as the FRC excludes the flux in the translation region, so that for a constant flux conserver radius at least, the equilibrium $B_{z,eq}$ will increase.

For MTF applications we are faced with several constraints on the experimental design. These are:

1. The translation speed v_z must be fast enough so that for a given length for the translation region L_z, the FRC arrives at the target compression region in a time τ_{xltn} faster than its particle decay time given by τ_N.

2. The compressed magnetic field Bz must be significantly less than the compressed theta coil field so that translation speed v_z is sufficiently large and translation time $\tau_{xltn} = L_z/v_z \ll \tau_N$ is sufficiently small that the $\tau_{xltn} \ll \tau_N$.

3. The expanded FRC must fit inside the translation vacuum vessel

4. The expanded FRC must have sufficient kinetic energy to get into the liner region and fit inside it.

As the guide field was decreased in FRX-C/LSM, the FRC was observed to accelerate, cool, and expand. The FRX-C/LSM data spans a range for formation to translation field of $0.5 < B_{z2}/B_{z1} < 1$. In FRX-C low compression experiments, the normalized separatrix radius x_s was measured as it increased, and these data were used to verify the relations laid out in section IV.C Adiabatic scaling of the FRC parameters has worked well in the past for predicting translation parameters for other experiments as well (Tanjyo et al., 1984) (Tuszewski, 1988b).

The foregoing assumptions that energy, flux and particles are conserved can be adjusted using the measured confinement lifetimes for these quantities.

B. MTF Design example

1. Fit the FRC into translation radial boundary

In order to minimize the plasma expansion and cooling as predicted by equation 16, we wish to maintain the FRC radius r_{s2} to be no larger than the formation r_{s1}. For our initial experiments, we have selected a conical theta coil half angle $\alpha = 2$ degrees, a value for $B_{z2}/B_{z1} \approx 0.7$, and $x_{s2} \approx 0.45$ is then determined from figure 2.

A survey of a range of flux conserver boundary radii is shown in figure 8

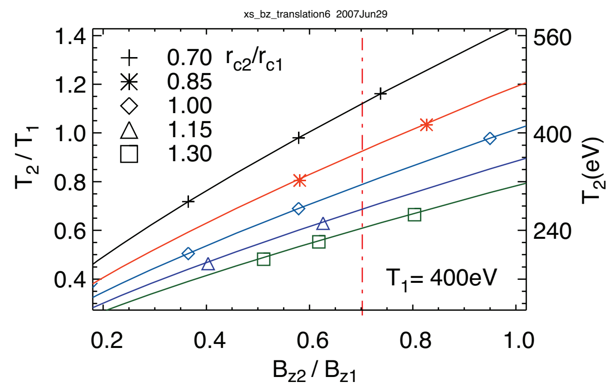

FIG. 8 Model predictions for temperature of translated FRC for a range of flux conserver radius ratios $0.7 < r_{c2}/r_{c1} < 1.3$.

If the translation region flux conserver radius is smaller than the average θ coil radius, then the expansion and cooling can be reduced. For instance if the formed FRC has $r_s 1 \approx 2.5$cm, and the design point is at $B_{z2}/B_{z1} = 0.7$ then the required translation flux conserving boundary would be $r_c = 5.6$cm to maintain the translating FRC at the same radius r_{s2} as the average r_{s1} during formation.

There is still an open question whether or when the FRC rethermalizes translation energy when it slows down as predicted by the Ohi equation 17. The entropy constraint, for a thermodynamic series of changes is $ds = dH(1/T_2 - 1/T_1) = dH(T_1 - T_2)/(T_1T_2)$ where s is entropy, H is enthalpy, T is temperature, and $ds > 0$ for irreversible processes. If the Ohi equation is not reversible, then an equivalent statement would be that enthalpy is not conserved, and the pre requisite adiabatic assumptions are not valid. This could result from losses, accelerations or compressions that occur on time scales that are comparable to Alfven or ion acoustic transit times.

For the arguments made in this paper, the worst case assumption for translation and reflection is that the reheating is zero, and that losses occur on time scales that are discussed in section VI.B.3. Reversibility and reheat would be likely if the entropy change is zero. This would follow from adjustment of the magnetic field, geometry, or vacuum field such that T_2 is never smaller than T_1.

2. Liner compression before FRC entry

For the SHIVA-Star facility the time required for liner compression to the final stagnation radius (Intrator et al., 2002) approximately 25μsec (Degnan et al., 2004). This is of the same order or even longer than the FRC lifetime τ_{FRC}. During the dynamic liner experiment, the liner implosion must be triggered prior to the FRC formation, and the liner radius at the time of FRC entry will be approximately 70% of the average θ coil radius $r_{c1} \approx 5.6$cm. The effective boundary radius will then be approximately $r_{c2}/r_{c1} \approx 0.7$.

Due to flux conservation, the imposed liner magnetic field will be compressed and thus magnified by a factor or 2. Therefore the field in the liner must be reduced so that it has the value $B_{z2}/B_{z1} \approx 0.7$ at the appropriate time during MTF compression.

In terms of FRC parameters we can account for the change in r_{c2}/r_{c1} Table I, or the example of figure 8.

After the FRC enters the liner, the compression due to the moving flux conserver radial boundary proceeds at constant x_s, and is beyond the scope of this study.

3. Translation *v.s.* FRC lifetime

Since the time required for translation is a significant fraction of the FRC lifetime, some fraction of the plasma particles and flux will be lost by the time the FRC reaches the liner. A decrease in internal poloidal flux will lead to a decrease in the normalized radius

$$x_s = \sqrt{2}\left(\frac{\phi_p}{\pi r_c^2 B_{eq,w}}\right)^{1/(3+\epsilon)} \quad (23)$$

as per equation 12. For example, with a pessimistic estimate that 50% of the flux is lost, then x_s would decrease by approximately 20%.

Using the design point of $B_{z2}/B_{z1} = 0.7$, we show in figure 9 a plot of the expected separatrix radius x_{s2}/x_{s1} as a function of the fraction of poloidal flux remaining. These are calculated for the translated FRC with a range of flux conserver radius ratios $0.7 < r_{c2}/r_{c1} < 1.3$, which could correspond to a radially converging flux conserver in the MTF compression region. To estimate the effects of changing the magnetic guide field, the lowest order approximation indicates that one can approximately scale the vertical axis $x_{s2}/x_{s1} \propto [B_{z1}/B_{z2}]^{1/(3+\epsilon)}$ for plot 9. An increase in B_{z2} will decrease x_{s2}/x_{s1}, but the dependence from equation 23 is weak.

Accumulated flux loss will decrease the amount of FRC plasma or flux that collides with the bore of the entrance throat for the deformable liner.

VII. DISCUSSION

The impending physics demonstration of MTF will utilize an FRC compact toroid magnetized plasma that will be translated into an imploding metal flux conserving boundary that will then compress the plasma. We have applied a physics model that only invokes general equilibrium and few dynamic assumptions to the design of a translating FRC experiment. We use an adiabatic model, and presume that the FRC plasma evolves through a sequence of isentropic magnetohydrodynamic (MHD) equilibria. This is a thermodynamic approach that only accounts for initial and final states and omits dynamics. For prolate FRC's, elongated equilibria are a reasonably description, and this property enables one to extract two dimensional information from a one dimensional calculation We consider adiabatic compressions of the idealized cylindrical FRC that can occur either via changes in wall compression or flux compression. The compressed equilibrium field is related to the applied magnetic field that must be furnished with external magnets, and an engineering figure of merit is quantified for use in the design procedure. The translation speed and energy are estimated, and design compromises between conflicting robust formation and maximum speed are discussed. For the translation part of an integrated MTF liner on plasma experiment, a design example is outlined.

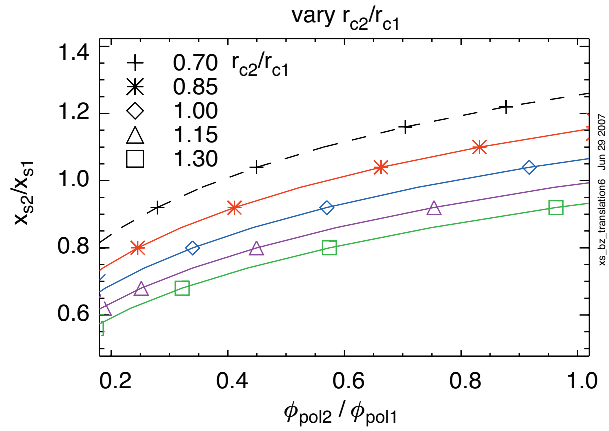

FIG. 9 The final separatrix radius x_{s2}/x_{s1} is compared with its formation value for arbitrary fractional flux losses between zero $0 < \phi_{pol,2}/\phi_{pol,1} < 1$ and unity. These are calculated for the translated FRC with a range of flux conserver radius ratios $0.7 < r_{c2}/r_{c1} < 1.3$.

In light of the foregoing considerations, the design point for the experiment has been selected to be B_{z2} in the translation region to be approximately 70% of the average field in the formation theta coil $B_{z2} \approx 0.7B_{z1}$. For the near term experiments, the maximum formation field at the narrow end of the conical θ coil is set to approximately 4 Tesla. The translation speed v_{z2} is estimated to approach the upstream source ion acoustic speed. Increased trapped flux during formation will be helpful for this entire exercise. Consequent larger temperature will increase v_{z2} and the flux remaining at moment of liner MTF compression.

This approach is shown to be useful for selecting the hardware capabilities and operating point for a high density FRC that must be propelled into a Magnetized Target Fusion compression region.

Acknowledgments

This work was supported by the Office of Fusion Energy Sciences at Los Alamos National Laboratory, U.S. Department of Energy under LANS Contract No. DE-AC52-06NA25396.

References

R. C. Kirkpatrick, I. R. Lindemuth, and M. S. Ward, Fusion Technology **27**, 201 (1995).

T. Intrator, S. Y. Zhang, J. H. Degnan, I. Furno, C. Grabowski, S. C. Hsu, E. L. Ruden, P. G. Sanchez, J. M. Taccetti, and M. Tuszewski, Physics of Plasmas **11**, 2580 (2004a).

S. Y. Zhang, G. A. Wurden, T. P. Intrator, E. L. Ruden, W. J. Waganaar, C. T. Grabowski, R. M. Renneke, and J. H. Degnan, IEEE Transactions On Plasma Science **34**, 223 (2006).

R. E. Siemon, I. R. Lindemuth, and K. F. Schoenberg, Comments Plasma Phys. Control. Fusion **18**, 363 (1999).

T. Intrator, M. Nagata, A. Hoffman, H. Guo, L. Steinhauer, D. Ryutov, R. Miller, and S. Okada, Journal of Fusion Energy **23**, 175 (2004b), article Journal article Review 0164-0313 10.1007/s10894-005-5597-9 Copyright 2006 Elsevier Engineering Information, Inc.; IEE; The Thomson Corporation.

D. J. Rej, W. T. Armstrong, R. E. Chrien, P. L. Klingner, R. K. Linford, K. F. McKenna, E. G. Sherwood, R. E. Siemon, M. Tuszewski, Milroy, et al., Phys. Fluids **29** (1986).

W. T. Armstrong, R. K. Linford, J. Lipson, D. A. Platts, Sherwood, and G. E, Physics of Fluids **24**, 2068 (1981).

J. T. Slough and A. L. Hoffman, Proceeding Series of the International Atomic Energy Agency (1997).

K. Wira and Z. A. Pietrzyk, Physics of Fluids B (Plasma Physics) **B**, 561 (1990).

H. Y. Guo, A. L. Hoffman, L. C. Steinhauer, and K. E. Miller, Physical Review Letters **95** (2005).

R. L. Spencer, M. Tuszewski, and R. K. Linford, Phys. Fluids **26**, 1564 (1983).

M. Tuszewski, Physics of Fluids **31**, 3754 (1988a).

H. Grad, P. Hu, and D. Stevens, Proc. National Acad. Science, USA **72**, 3789 (1975).

R. Byrne and W. Grossmann, Proceedings of the Third Symposium on Physics and Technology of Compact toroids in the magnetic fusion Energy Program p. 138 (1980).

M. Tanjyo, S. Okada, Y. Ito, M. Kako, S. Ohi, S. Goto, T. Ishimura, and H. Ito, Technology Reports of the Osaka University **34** (1984).

D. W. Hewett and R. L. Spencer, Physics of Fluids **26** (1983).

D. C. Barnes, C. E. Seyler, and D. V. Anderson, in *Compact toruses and energetic particle injection* (Princeton Plasma Physics Laboratory, Princeton Plasma Physics Laboratory, 1979), p. 110.

H. Himura, Y. Suzuki, S. Ueoka, H. Taniguchi, M. Okubo, S. Sugimoto, S. Okada, and S. Goto (Sao Jose des Campos, Brazil : INPE, 1994, 1994).

M. Tuszewski, Nucl. Fusion **28**, 2033 (1988b).

M. Tuszewski, Phys. Fluids **24**, 2126 (1981).

R. D. Milroy and J. U. Brackbill, Physics of Fluids **29** (1986).

D. Wells, Phys of Fluids **9**, 1010 (1966).

D. Wells, E. Nolting, F. Cooke, J. Tunstall, P. jindra, and J. Hirschberg, Phys Rev. Letters **33**, 1203 (1974).

M. Tuszewski and B. L. Wright, Physical Review Letters **63** (1989).

R. E. Chrien and W. T. Armstrong, Bull. Am. Phys. Soc. **29**, 1328 (1984).

K. Kawai, Ph.D. thesis, Univ. Washington (1987).

W. Armstrong and R. D. Milroy, in *Symposium on physics and technology of compact toroids in the magnetic fusion energy program*, Los Alamos National Lab., NM (USA) (Los Alamos National Lab, 1982), vol. LA-UR-82-3443 of *CONF-821124-5*.

T. Intrator, M. Taccetti, D. A. Clark, J. H. Degnan, D. Gale, S. Coffey, J. Garcia, P. Rodriguez, W. Sommars, B. Marshall, et al., Nuclear Fusion **42**, 211 (2002), article Journal article 0029-5515 Copyright 2006 Elsevier Engineering Information, Inc.; IEE; The Thomson Corporation.

J. H. Degnan, D. Amdahl, A. Brown, T. Cavazos, S. K. Coffey, G. G. Craddock, M. H. Frese, S. D. Frese, D. Gale, T. C. Grabowski, et al. (Piscataway, NJ, USA : IEEE, 2004, 2004).